JUPITER'S RADIO EMISSION AND SOLAR ACTIVITY

C. H. Barrow

Groupe Decametrique, Observatoire de Meudon,
92195 Meudon, France[1]

Abstract

Observations of the solar wind velocity, density, and pressure, and the interplanetary magnetic field (IMF) magnitude close to Jupiter are compared with the decametric (DAM), the hectometric (HOM), and the broad–band kilometric (bKOM) components of the Jovian radio emission observed by Voyager. Some measure of solar wind control is found to exist in each case although each radio component is differently correlated with the solar wind. At decametre wavelengths the results support those obtained several years ago, using ground–based observations, in that only the non–Io DAM is found to be influenced by solar activity; the Io–DAM does not show any degree of solar control. The IMF magnitude, the solar wind density, pressure and velocity are all found to correlate with the non–Io DAM. Both the bKOM and the HOM are influenced to some extent by the IMF magnitude and the solar wind density and pressure but not by the solar wind velocity. There are indications that all three radio components are somehow associated with interplanetary magnetic sector structure although the exact nature of the relationship remains obscure.

1. Introduction

This review paper surveys the following topics. In the next section, the first indications of solar influence on ground–based observations of the DAM are outlined briefly, leading to the general conclusion that the non–Io DAM is in some manner influenced by the IMF sector structure. Section 3 summarizes the Voyager Planetary Radio Astronomy (PRA) experiment, the radio and solar wind data sets available and the techniques that have been used for their analysis. Sections 4, 5, and 6 outline the results obtained for the DAM, the HOM, and the bKOM, respectively. These results are discussed and summarized in Section 7.

2. Pre–Voyager DAM observations

The DAM was discovered accidentally in 1954 by Burke and Franklin (1955b). In the years following this discovery, statistical techniques established the existence of "sources" or regions of relatively high occurrence probability in Central Meridian Longitude (CML). In 1964, Bigg (1964) discovered that many of the DAM noise storms were closely correlated with the position of the Galilean satellite Io relative to the Earth–Jupiter line. Both of these two effects were originally demonstrated by occurrence probability histograms which

[1]Present address: MPI für Aeronomie, Postfach 20, D–3411 Katlenburg–Lindau, F.R.G.

were later superceded by three–dimensional plots of the type shown in Figure 1 (Thieman, 1979). The terms Io– and non–Io emission were adopted to refer, respectively, to DAM that was correlated or not correlated with the position of Io expressed by its geocentric longitude.

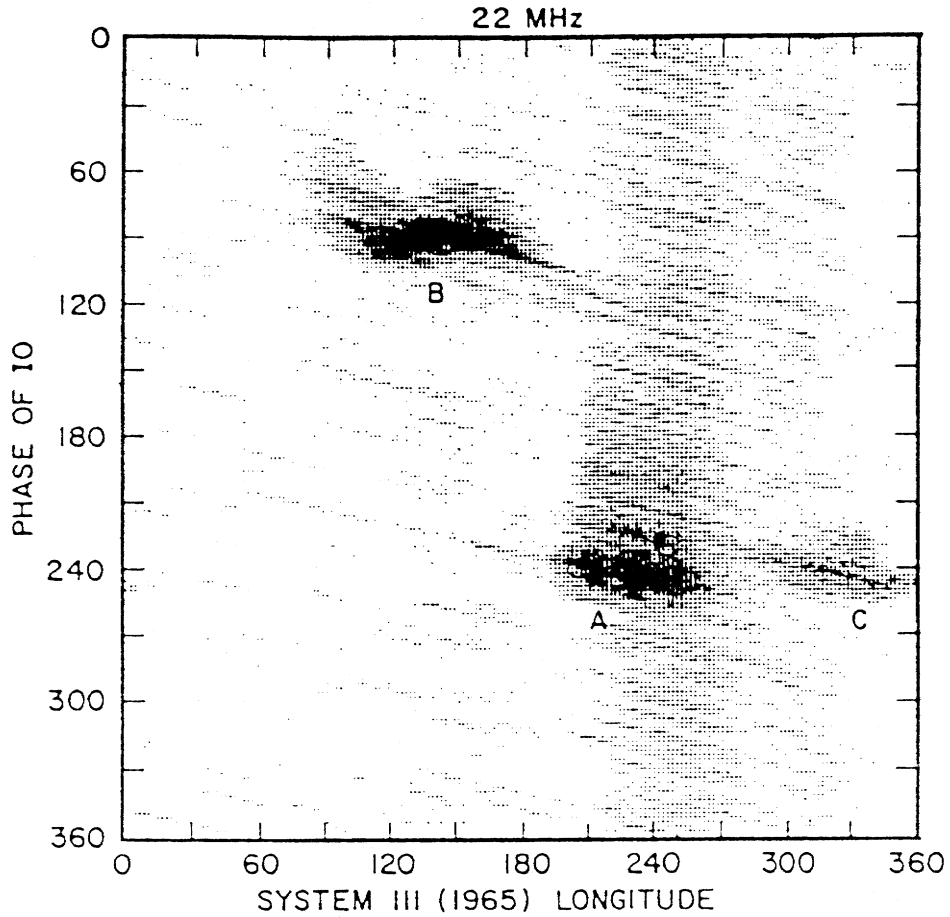

Fig. 1: DAM events plotted by CML and Io–phase, for fixed–frequency observations at 22 MHz from 1958 through 1975 (Thieman, 1979).

Soon after the discovery of the DAM, Carr et al. (1958) noted that the most intense DAM noise storms seemed to occur at roughly 7– to 8–day intervals (Figure 2a). The Io effect was still not known when Carr et al. (1960) later suggested that the DAM might be an effect of "solar particles" incident upon the upper atmosphere of Jupiter. On the assumption that these particles would disturb the Earth's magnetic field as they passed by on their way to Jupiter, Carr et al. (1961) suggested the existence of a systematic lag of some 8 days between periods of enhanced geomagnetic activity and DAM events (Figure 2b). Although this apparent lag was later found to be due to two periodicities, both involving the revolution period of Io, (Sastry, 1968; Barrow, 1985) these ideas opened the way for future research where the solar particles came to be identified with the solar wind.

A search for possible short–term correlation between solar activity and the DAM observed

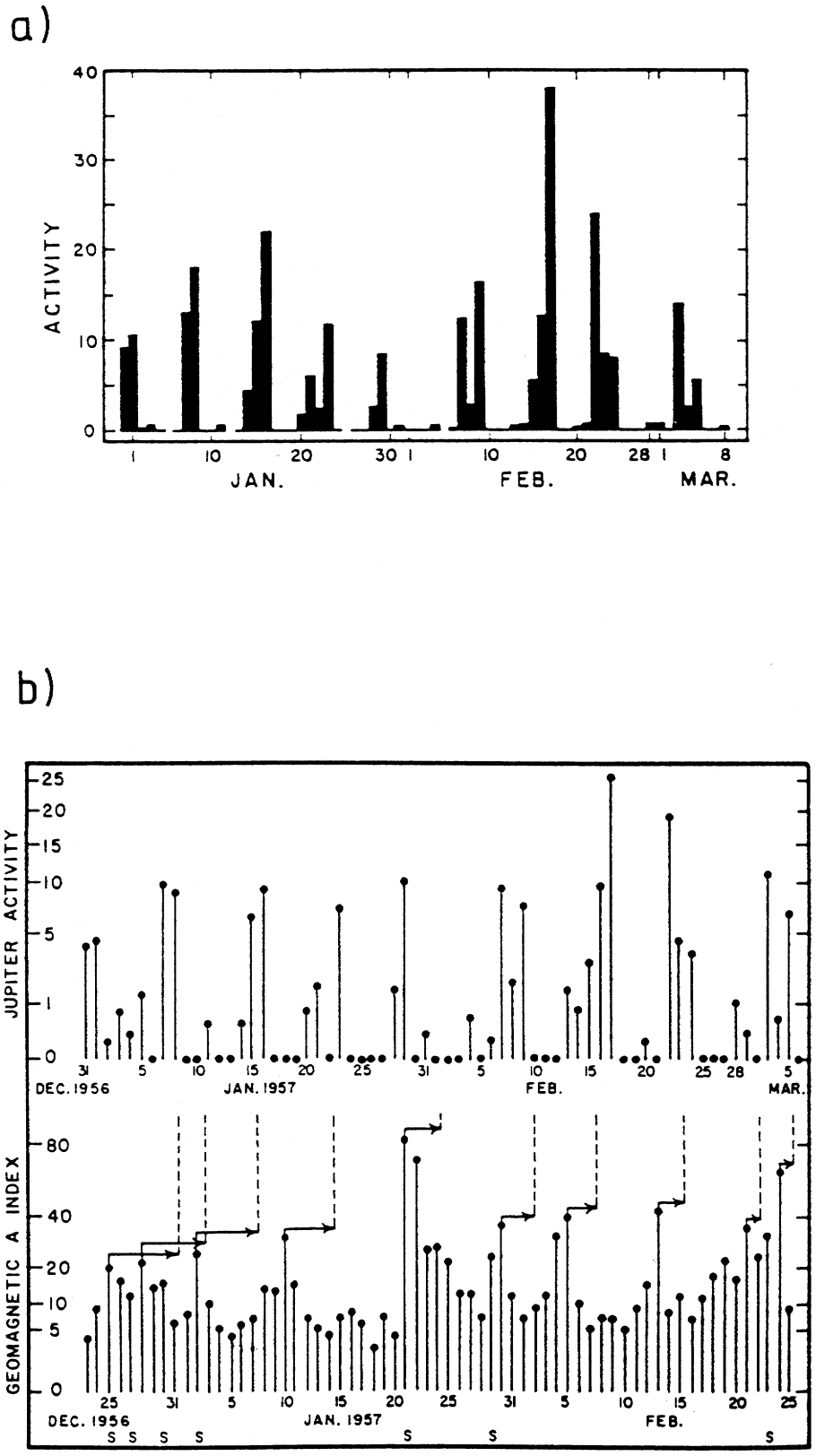

Fig. 2: (a) Daily Jovian activity showing the 8–day periodicity (Carr et al., 1958). (b) Comparison of the geomagnetic A_p index with a daily Jupiter activity index, for 18 MHz observations in 1957. The time scale for the A_p index has been advanced 8 days relative to the Jupiter activity time scale (Carr et al., 1961).

at the Earth inevitably makes the assumption that something (i.e. the solar wind) affects the Earth (i.e. the magnetic field) as it passes on its way to Jupiter where the DAM is somehow triggered. Even if this simple model were completely true it would only be precisely realized close to opposition for particles travelling with uniform and constant radial velocity. A number of complicating factors exist, however. These have been considered in studies by Sastry (1968), Douglas and Bozyan (1970), Kovalenko (1971), and Barrow (1972). The problems have been reviewed in some detail by Barrow (1985); they may be summarized briefly as follows:

1. Changing Earth–Sun–Jupiter geometry.
2. Possible beaming of solar–activated DAM in directions away from the Earth.
3. Intermittent periods of DAM data.
4. Possibility of both solar–correlated and uncorrelated types of DAM.
5. Solar particle velocity variations.
6. Artificial periodicities in the data which may indicate spurious correlations.

Compromise methods were developed (Barrow, 1978, 1979) in an attempt to minimize the effects of these problems. Using the method of superposed epochs (Chree, 1912), with DAM events as epochs against continuous values of the geomagnetic A_p index as an indicator of solar activity, Barrow (1979) showed (Figure 3) that, for the period 1960 through 1977, the non–Io DAM was correlated with variations of A_p while the Io–DAM showed no indication of correlation. The data were separated into non–Io DAM events before and after opposition so that the positional lags of the correlation peaks, which correspond to prevailing solar wind average velocities, could support the argument if the lags were physically plausible. While the peak in the After Opposition analysis was obviously consistent with this idea, the Before Opposition peak, at first sight, appeared to lack physical plausibility. To explain this, Barrow (1979) pointed out that for typical solar wind velocities of some 350 to 400 km/s it was possible for the corresponding Archimedean spiral, or corotating interaction region (CIR), to encounter both the Earth and Jupiter at about the same time (Figure 4). This lead to the suggestion that the non–Io DAM was either directly or indirectly associated in some manner with interplanetary magnetic sector structure. Superposed epoch analyses for the non–Io DAM observed during the years 1962–64 and 1974, when the sector structure was exceptionally stable for long periods, showed that the correlation effects were much enhanced for these periods. These results were consistent with the findings of Kennedy et al. (1974), Oya and Morioka (1977), Terasawa et al. (1978), Levitskii and Vladimirskii (1979), and Pokorny (1982), all of whom reached similar conclusions from somewhat different arguments. Thus, at the time of the Voyager Jupiter encounters in 1979, a fair measure of agreement had developed concerning the influence of the Sun upon the DAM.

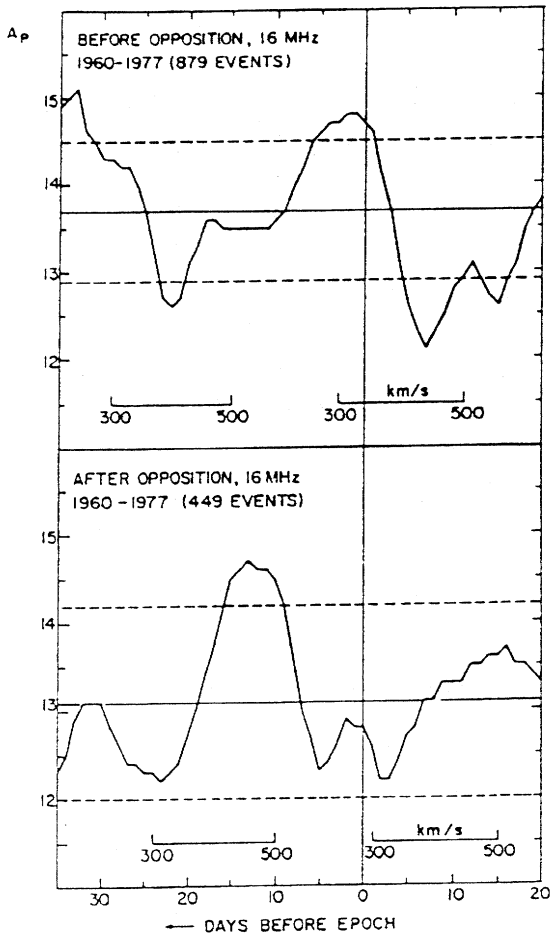

Fig. 3: Superposed epoch analyses of non–Io DAM against the geomagnetic A_p index for 16 MHz data from 1960 through 1977. The broken lines indicate 99% confidence levels.

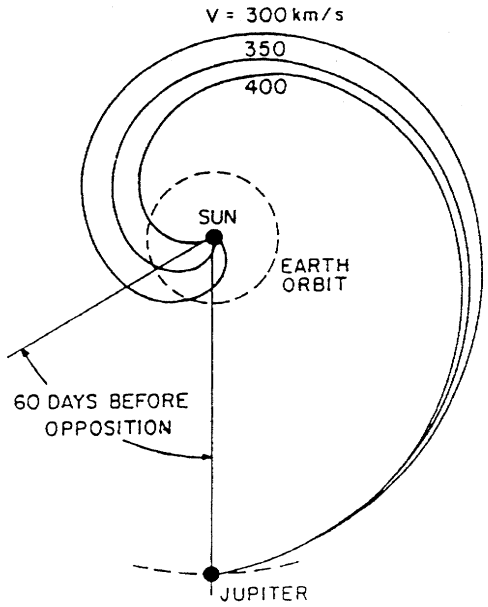

Fig. 4: Idealized solar wind velocity spirals that could produce coincidences or negative delays during the 60–day period immediately before opposition.

3. Data sets and analysis methods

The Voyager PRA receiver operates in two bands, high band (from 1.3 to 40 MHz) and low band (from 1.2 to 1300 kHz). Each band is scanned in steps and so integrated energy values for a specific period and frequency range are readily available. Typical dynamic spectra (Figures 5a and 5b) show the presence of three distinct components in addition to the DAM; a hectometre–wavelength emission (HOM) and two kilometre–wavelength components, broad–band (bKOM) and narrow–band (nKOM). The PRA experiment and the characteristics of each of these components have been reviewed by Alexander et al. (1981), by Boischot et al. (1981), and by Carr et al. (1983). Each radio data set will be described under the appropriate Sections 4, 5, and 6.

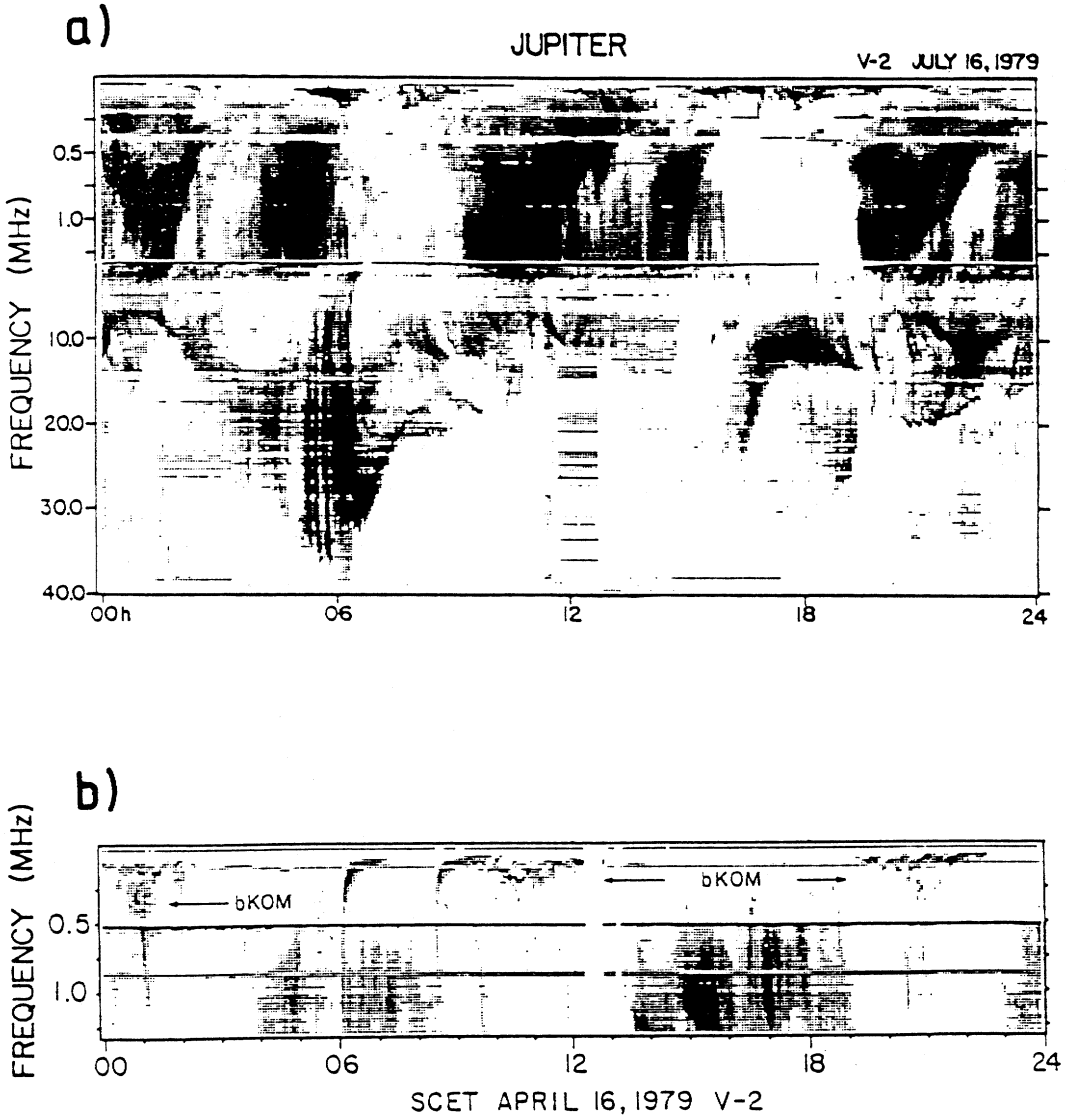

Fig. 5: 24–hr frequency–time dynamic spectra from the Voyager 2 PRA experiment, (a) comparing HOM emission with DAM and KOM activity on July 16, 1979 and (b) showing the bKOM on April 16, 1979 (Kaiser and Desch, 1984).

Solar wind data were taken by the Plasma Science (PLS) experiment (Bridge et al., 1977), interplanetary magnetic field data by the Magnetometer (MAG) experiment (Behannon et al., 1977) and radio data by the PRA experiment (Warwick et al., 1977). Short gaps in the solar wind data can be covered by interpolation, longer gaps have to be avoided. Thus the selection of suitable periods for study is sometimes a matter of compromise. For example, solar wind observations could not be made when a spacecraft was in the Jovian magnetotail.

Several methods have been used, as appropriate, in the search for correlation effects. These are as follows:

1. Comparison of time series.
2. Power spectrum analysis.
3. Auto correlation.
4. Cross correlation.
5. Superposed epochs.

Examples of each of the above are mentioned in the following sections, although (4) and (5) have proved to be the most useful. We note that for cross correlation it is necessary to have two continuous time series for comparison, whereas the method of superposed epochs can set a discontinuous data set (in this case the radio data) against a continuous data set (a solar wind parameter or the IMF magnitude). Cross correlation is relatively simple, although the data may need filtering to allow for the different characteristic durations of periods of enhancement in each of the two time series. We shall see that confirmation of the results may sometimes be obtainable from auto correlation if the data sets are sufficiently long. On the other hand, radio event selection by various criteria is uncertain in cross correlation while it is easy and objective with the method of superposed epochs.

Each of the radio components, the DAM, the HOM, and the bKOM have been compared, separately, with the IMF magnitude and with the solar wind density, pressure and velocity. The results are presented separately for each radio component in the following three sections.

4. DAM

The Voyager DAM data were taken by the PRA high–band receiver. In addition to the integrated energy values available, Barrow (1981) has catalogued the DAM events above 15 MHz, defined by spectral extent in the time–frequency plane, in a format which closely follows that established by Warwick et al. (1975) for Earth–based observations of the DAM. A more recent catalogue by Aubier and Genova (1985) lists the events within the range 7 to 40 MHz, specifying the activity by the maximum frequency of emission within each successive 15° band of CML. The amount of Voyager DAM data is somewhat limited

due to the relatively low sensitivity of the PRA high–band receiver. Suitable data are available for some 25 days prior to each encounter, however, when coverage is close to 100% for both the radio and the solar wind data. The method of superposed epochs was adopted in order to combine the Voyager 1 and the Voyager 2 two data sets. The results are summarized in Figures 6 and 7. A more detailed account has been given elsewhere by Barrow et al. (1986).

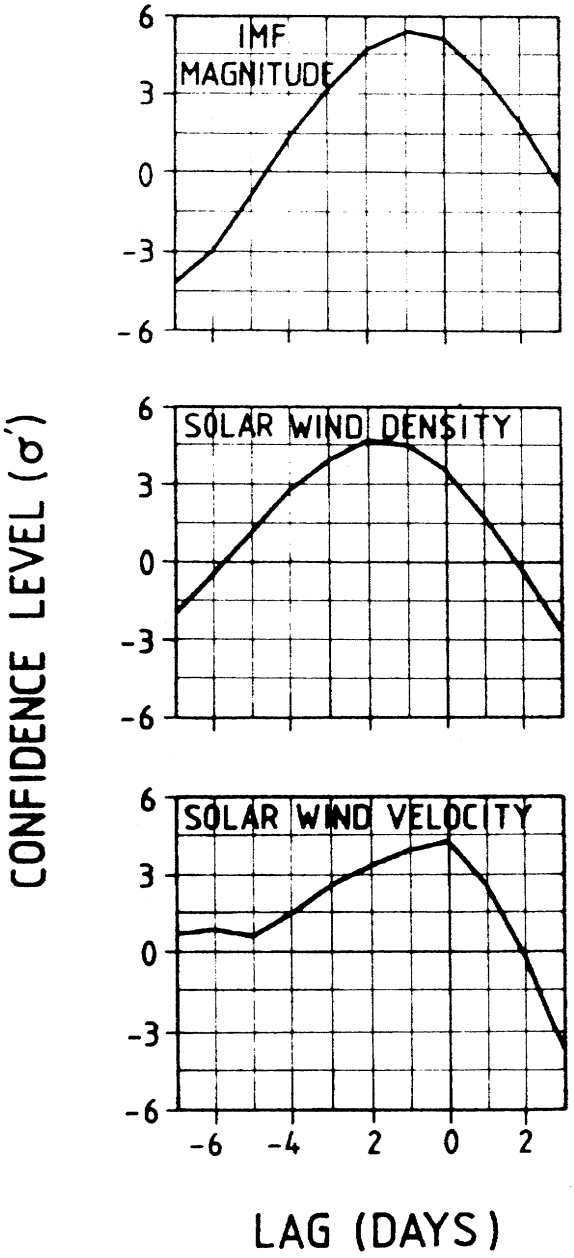

Fig. 6: Superposed epoch analyses of the combined non–Io DAM observed by both Voyager 1 and Voyager 2 during the periods preceeding each encounter.

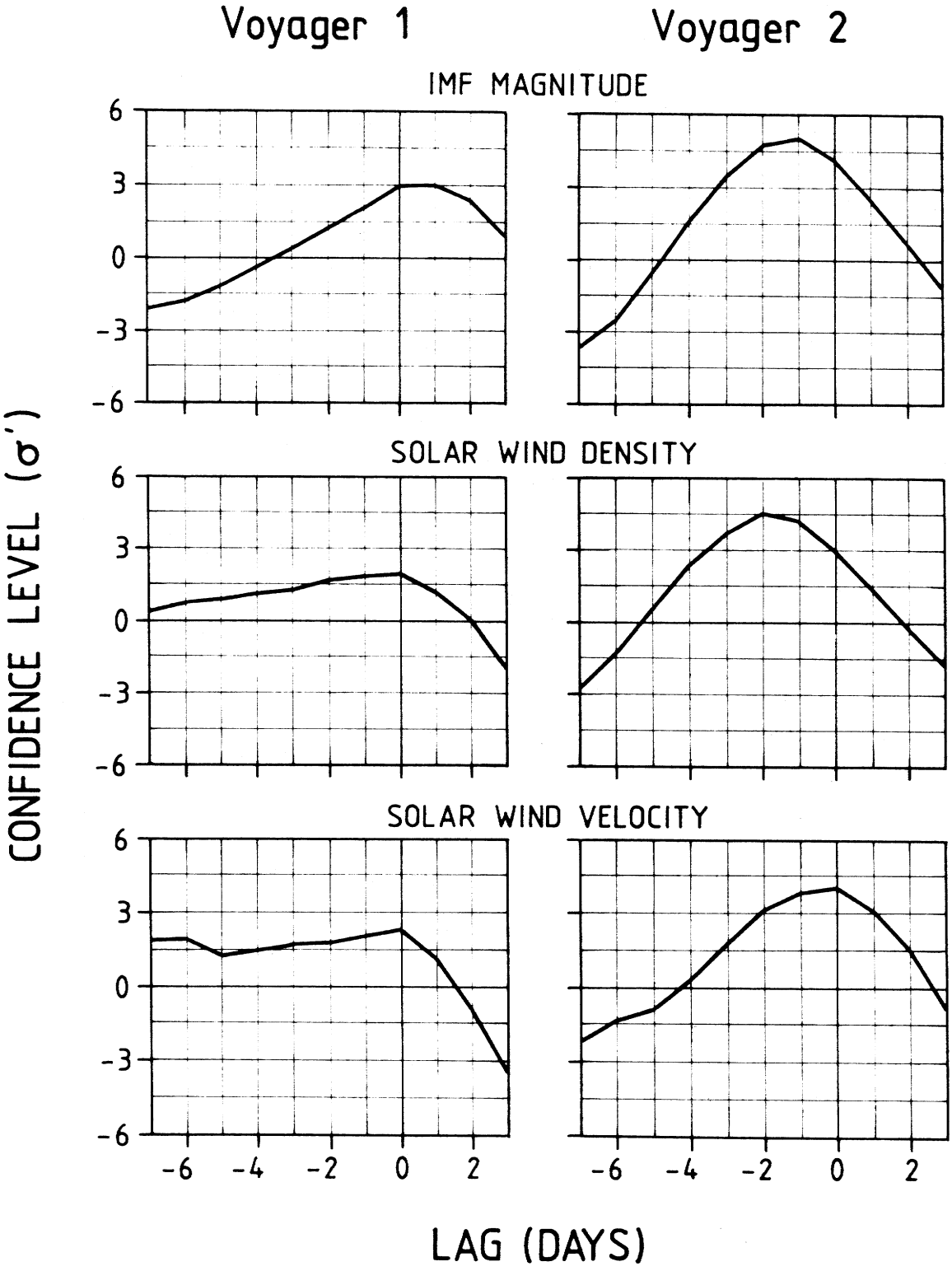

Fig. 7: Separate superposed epoch analyses of the non–Io DAM observed before each encounter by Voyager 1 and by Voyager 2.

Superposed epoch analyses of the combined Voyager 1 and Voyager 2 data are shown in Figure 6. Each figure has been normalized by expressing the correlation in terms of σ' a "modified standard error" (MSE) which defines the confidence level according to the usual criteria (Bell and Glazer, 1958; Barrow, 1972). Thus three MSE define a 99.7% confidence level. It can be seen that, for the non–Io DAM, highly significant correlation (better than four MSE) is found with the solar wind density and the solar wind velocity as well as with the IMF magnitude. The solar wind pressure results, which are not shown here, closely follow those for density, as might be expected. If the Voyager 1 and Voyager 2 data are examined separately, however, we find (Figure 7) that the correlation, shown in Figure 6, is almost entirely due to the Voyager 2 data. There is no suggestion of a correlation effect for the Io DAM in any of these cases.

The results presented in Figures 6 and 7 have been calculated by selection of non–Io events from the Aubier and Genova (1985) catalogue. Similar results are obtained for non–Io events selected from the Barrow (1981, 1985) catalogue when the corresponding confidence levels are lower although still significant at a level of three MSE.

Cross correlation, as described for the HOM in Section 5, can only be calculated for continuous data sets and this restricts the technique to separate examination of the Voyager 1 and Voyager 2 pre–encounter periods. Taking the radio parameter as average energy per rotation (10–hr) over a frequency band 16.4 to 19.7 MHz, correlation is found to be quite good for the DAM and the solar wind velocity observed by Voyager 2 but only marginal for the corresponding Voyager 1 observations. Non–significant results were obtained for the IMF magnitude and for the solar wind density and pressure. In this case, however, all of the DAM is included, as non–Io event selection is not readily available for the energy averages. The time series were randomized in the manner, originally due to Desch and Rucker (1983), and adopted for the HOM by Desch and Barrow (1984) as in Section 5.

Clearly, cross correlation is a somewhat crude approach in the case of the DAM as the inclusion of Io events (some 40% of the total duration of emission above 15 MHz, according to Aubier and Genova, 1985) has a considerable effect on the result.

The superposed epoch analyses, presented in Figures 6 and 7, prompt us to ask, "What might be different for the two pre–encounter periods that could give rise to the well–defined correlation seen in the Voyager 2 data and the almost complete absence of correlation for the Voyager 1 data?" The two most obvious considerations that may be relative are (i) the trajectories of the two spacecraft as they approached Jupiter and (ii) the condition of the interplanetary medium, at the time of the observations.

The two spacecraft approached from Jovicentric declinations (D_E for an observer at the Earth) of about $+3°$ for Voyager 1 and about $+7°$ for Voyager 2. Beaming effects in the DAM are known to be critically dependant upon D_E (Carr and Desch, 1976) and so it may be that the difference in correlation for Voyager 1 and Voyager 2 is a result of the difference in D_E during approach. On the other hand, if we compare Earth–based observations of the DAM, the non–Io DAM was very strongly correlated with the A_p index throughout the apparitions of 1962 through 1964 and during the apparition of 1974. From

1962 to 1964, D_E increased from about +1.5° to +3°, in 1974 D_E was about +2°; in both cases D_E was less than or equal to the approach value for Voyager 1.

An alternative possibility is shown in Figure 8, where time profiles of the solar wind density, the IMF magnitude and the B_z component are compared for the six–month period preceeding Voyager 2 encounter. It can be seen that, for the last 60 days prior to encounter, from Day of Year 1979 (DOY) 120 through DOY 180, the IMF magnitude and the solar wind density both show a well–defined periodicity of some 13 days with corresponding sharp reversals of the B_z component, indicating a well–defined IMF sector structure which is not present during the period preceeding Voyager 1 encounter. This structure is also confirmed by the auto correlation curves shown in Section 5 for the HOM (Figure 10). It has already been seen, in Section 2, that the correlation effects for Earth–based observations could relate back to IMF sector structure; the results shown here for the Voyager DAM data may be a further manifestation of this.

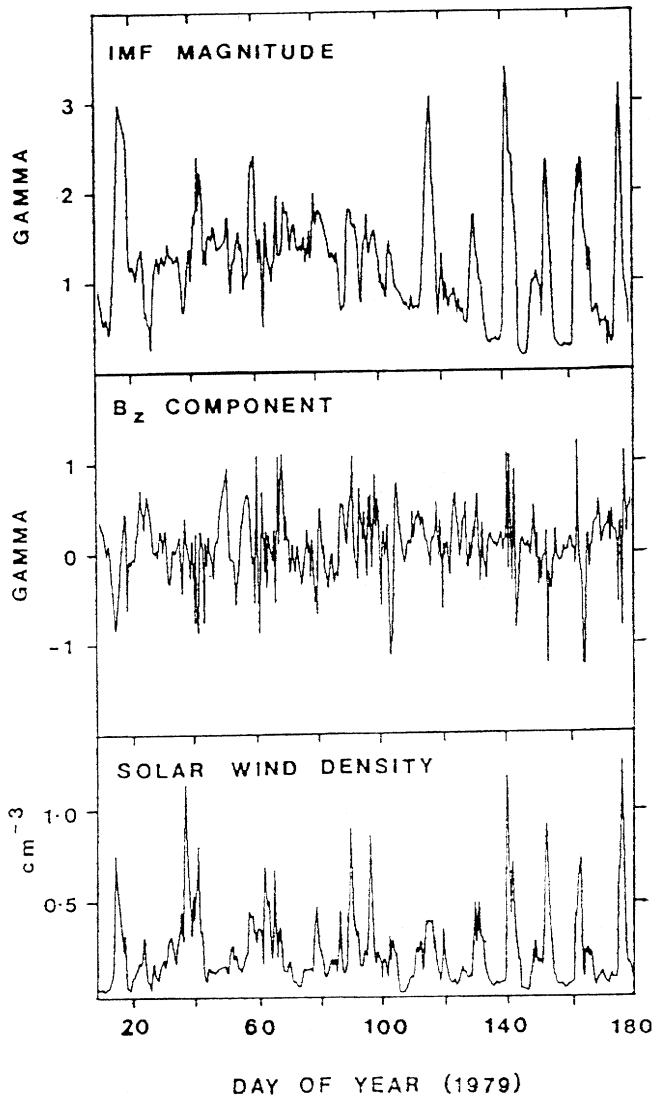

Fig. 8: Variation of the IMF magnitude, the B_z component and the solar wind density observed by Voyager 2 during the six–month period preceeding encounter.

We note also that the correlation effects are best demonstrated from the Aubier and Genova (1985) catalogue. In this catalogue, non–Io DAM is defined by spectral characteristics rather by the traditional CML and Io–phase criteria given by Carr and Desch (1976). As the Io DAM shows no indication of correlation, this may be an indication that it would advisable to re–define Io and non–Io emission in the manner suggested by Genova (1985), following Leblanc (1981) and further discussed by Aubier and Genova (1985).

5. HOM

The HOM extends from about 3 MHz down to about 100 kHz and it is, therefore, not observable from the Earth. It has been suggested by Lecacheux et al. (1980) that the HOM is a low–frequency extension of the DAM. There is, however, a distinct spectral peak close to 1 MHz (Brown, 1974) and the occurrence probability of the HOM, as a function of CML, differs from that of the DAM.

Zarka and Genova (1983) examined the power spectrum of the HOM and found several peaks common to both Voyager 1 and Voyager 2 observations. Two peaks, close to 10.5 and 14.5 days, they suggested might be due to IMF sector structure at Jupiter and hence they inferred solar wind control of the HOM.

Desch and Barrow (1984), following Desch and Rucker (1983), investigated the linear cross correlation between HOM energy and the solar wind density and velocity fluctuations at Jupiter (Figure 9) for periods, respectively, of 74 days and 173 days before the Voyager 1 and Voyager 2 encounters; that is, from December 18, 1978 (DOY 352) through March 1, 1979 (DOY 60) and from January 9 (DOY 9) through June 30, 1979 (DOY 181), respectively. In both cases, significant correlation (better than three standard deviations) was found between variations in the HOM energy and the solar wind density but not the velocity. The radio parameter is average HOM energy, per Jovian rotation (10–hr), of the total HOM observed by the PRA low–band receiver within a band of 500 to 1000 kHz. The solar wind variations are also 10–hr averages, projected ballistically from the spacecraft to Jupiter, in the manner described by Desch and Rucker (1983). Each time series was randomized before cross correlation (Jenkins and Watts, 1968) to eliminate the tendency, present in all data sets, for adjacent points in the same series to be highly correlated.

As a further test of the validity of the cross correlation, the non–randomized Voyager 2 solar wind density, velocity, and HOM profiles were auto–correlated to search for common periodicities (The corresponding Voyager 1 data were not available for a sufficiently long period to allow a lag of more than about 9 days). The results are shown in Figure 10 where it can be seen that both the HOM and the density curves have similar shapes up to some 18 days lag and both show similar peaks at about 13 days. Also, the "persistence times" (the width of the main peak from zero lag to the first zero crossing) are almost the same. The solar wind velocity auto–correlation curve does not match that for the HOM in either periodicity or persistence, however. Thus we conclude that the HOM and the solar wind density fluctuate on similar time scales while the solar wind velocity does not exert any appreciable control of the HOM.

Recent work by Barrow (unpublished) shows that, for Voyager 2 data, both the IMF magnitude and the solar wind pressure are also correlated with the HOM at a level of three standard deviations. Auto correlation gives curves consistent with those shown in Figure 10 for the HOM and the solar wind density. Superposed epoch analyses, using average HOM energies per Jovian (10–hr) rotation as epochs, confirm these results but also indicate that the correlation effects are mainly associated with the higher average HOM energies. The correlations are enhanced for the last two months prior to encounter, that is from DOY 120 through DOY 180. (Compare the results for the bKOM in Section 6).

As the solar wind density tends to increase along the leading edge of high speed streams, which are in turn related to IMF sector structure, these results seem to complement the association of non–Io DAM with sector structure previously suggested by Barrow (1979). They are also consistent with the results of Zarka and Genova (1983) who attributed 10.5 and 14.5 day periodicities in the HOM to IMF sector structure effects at Jupiter.

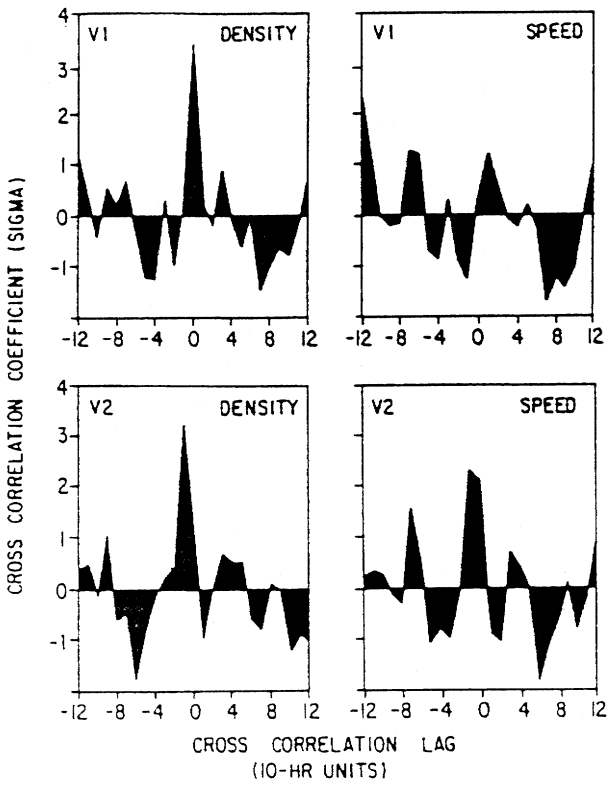

Fig. 9: Cross correlation coefficient, expressed in terms of standard deviation, against time–lag in Jovian rotations (10–hr) for HOM energy, correlated with solar wind density and with solar wind velocity, for both Voyager 1 and Voyager 2 data sets.

6. bKOM

The characteristics of the bKOM have been discussed in detail by Kurth et al. (1979), by Desch and Kaiser (1980) and, more recently, by Leblanc and Daigne (1985a). Although the emission can be observed from about 1000 down to 20 kHz it is mostly confined to frequencies below 500 kHz. Occurrence statistics, in terms of CML, show that this emission was observed predominantly in the CML range of about 120° to 270° when the spacecraft were at magnetic latitudes greater than 10°. There is no indication of bKOM control by Io although strong intensity modulations are sometimes observed from one rotation to the next.

Both Voyager 1 and Voyager 2 bKOM events have been catalogued by Leblanc (unpublished) in a format similar to that used by Barrow (1981) for his catalogue of DAM activity observed by Voyager, based upon the listings of Earth–based observations of DAM previously established by Warwick et al. (1975). For Voyager 2, radio data are also available in the form of 10–hour averages, over a bandwidth of 1 to 500 kHz. Both radio and solar wind data coverage are good for the periods selected for study, 60 days prior to Voyager 1 encounter from January 1 (DOY 1) through March 1, 1979 (DOY 60) and 160 days prior to Voyager 2 encounter from January 20 (DOY 20) through June 29, 1979 (DOY 180). A more detailed account has been given elsewhere by Barrow et al. (1988).

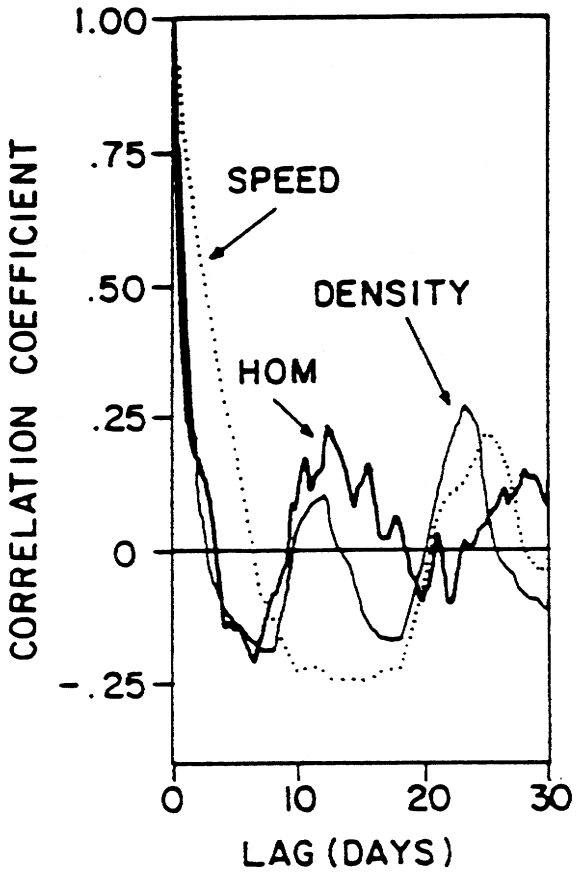

Fig. 10: Auto correlation coefficient versus time–lag in days for HOM energy, solar wind density and solar wind velocity, observed by Voyager 2.

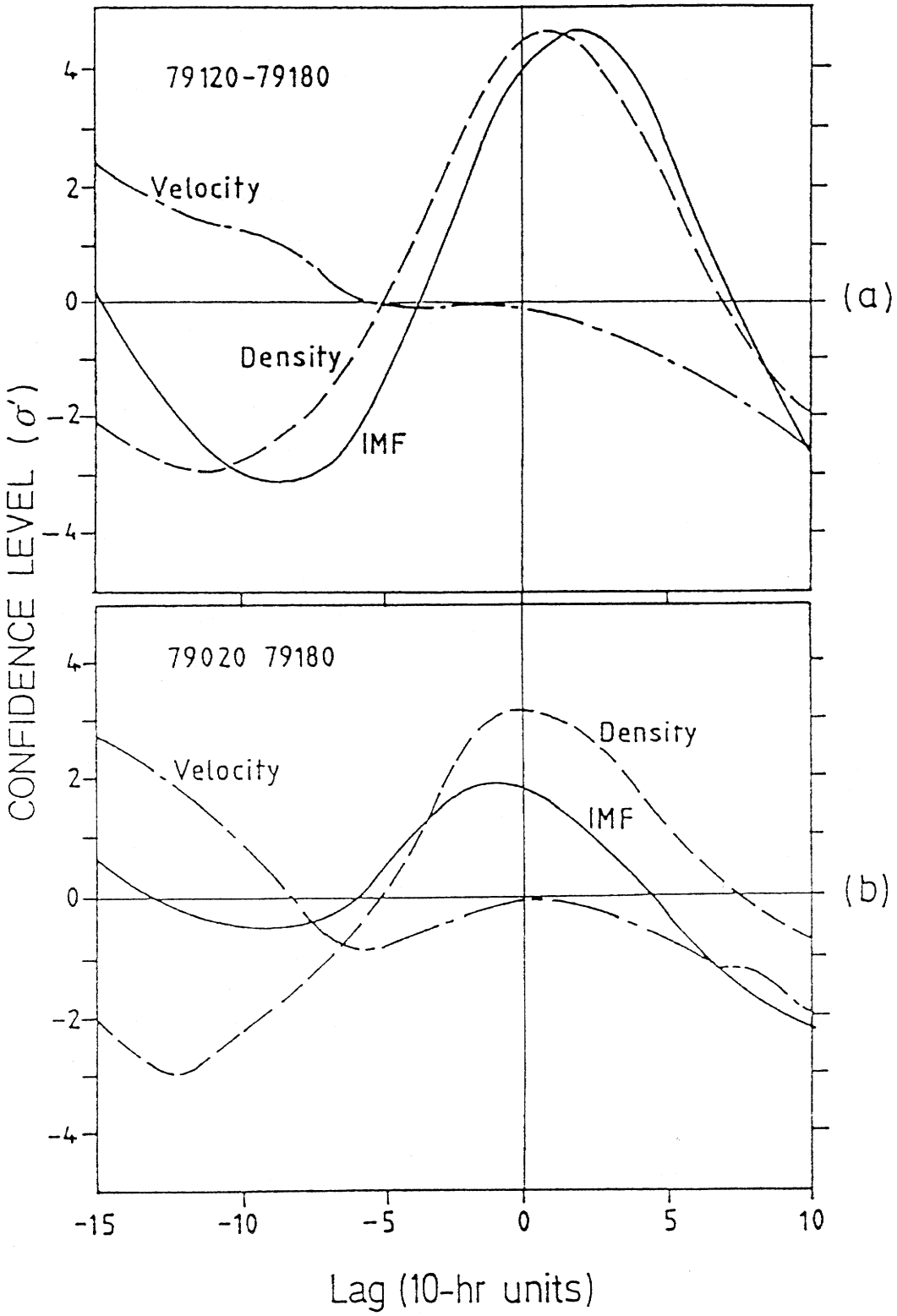

Fig. 11: Superposed epoch analyses of the lower frequency (20–310 kHz) bKOM events, (a) for the period DOY 120 through 180 and (b) for the period DOY 20 through 180.

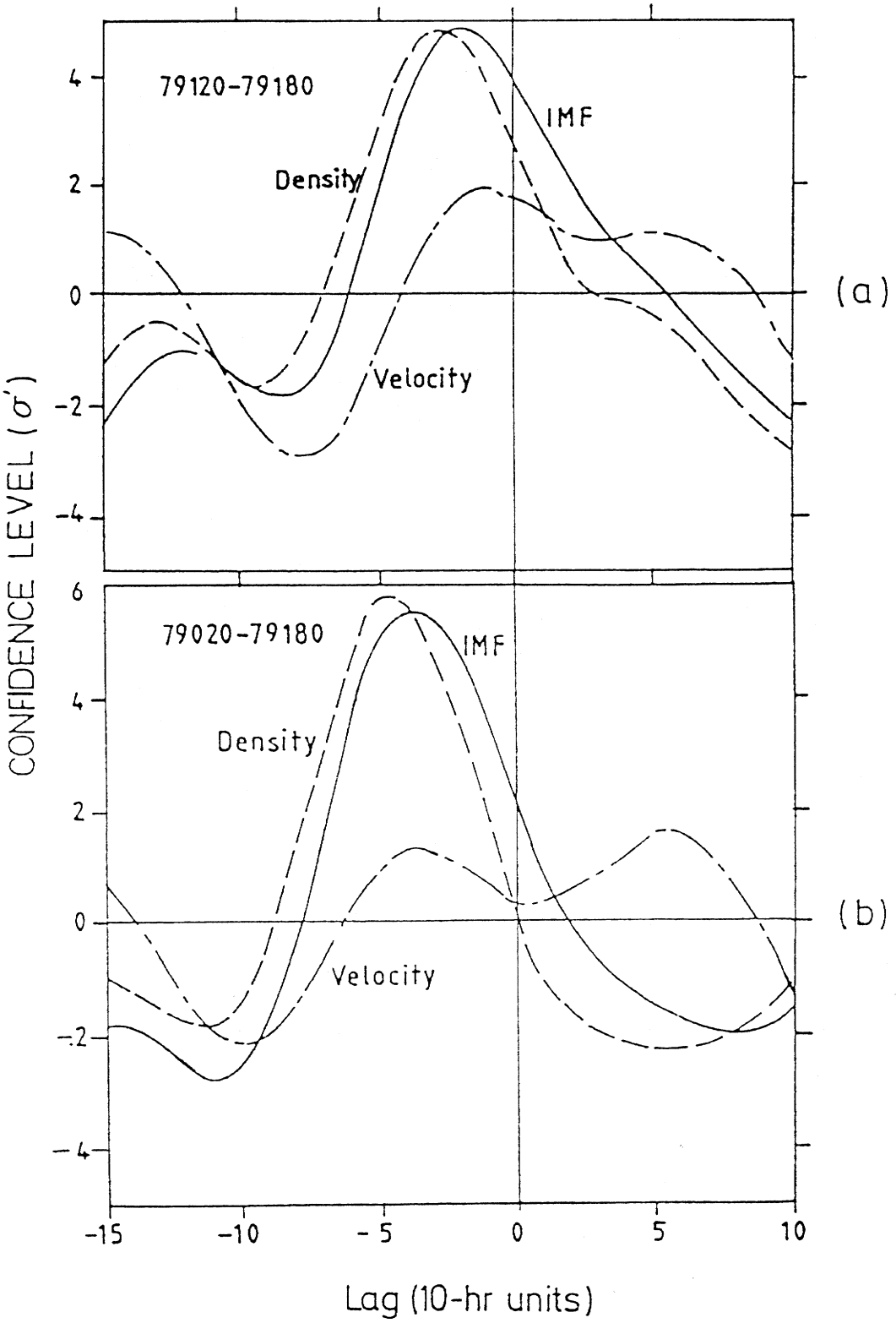

Fig. 12: Superposed epoch analyses of the lower average bKOM energies per rotation, (a) for the period DOY 120 through 180 and (b) for the period DOY 20 through 180.

The bKOM problem is more complex than that for either the DAM or the HOM. At first sight neither time series nor cross correlation reveal any significant correlation effects. However, the non–Io DAM, HOM, SKR (Saturnian kilometric radiation; Desch and Rucker, 1983) and the AKR (terrestrial auroral kilometric radiation; Gallagher and D'Angelo, 1981) all show correlation effects and so it might seem remarkable at first sight if the bKOM should not also be influenced in some manner by the solar wind. On the other hand, all of these other emissions are believed to originate in auroral regions while there are indications (Jones and Leblanc, 1987) that the bKOM source may be at the Io torus. If this is indeed the case, any possible solar wind effect should be comparable to that exerted on the terrestrial plasmasphere when, according to Gurnett and Frank (1976), it is compressed during periods of increasing magnetic activity.

A number of superposed epochs were computed, using as epochs Voyager 1 and Voyager 2 events selected from the Leblanc catalogue and Voyager 2 average energies/rotation. The period DOY 120 through DOY 180 was also examined separately in order to assess the possible effect of the prevailing IMF sector structure (Figure 8) during this period. Some of the results are shown in Figures 11 and 12 where, again, the analyses are normalized in terms of MSE.

In the case of the bKOM, only Voyager 2 data show any correlation effects and then only when the lower frequency (below 310 kHz) events (Figure 11) or the lower average energies (Figure 12) are selected for epochs. Energy correlation is then significant throughout the entire period DOY 20 through 180 while event correlation is only significant during the period DOY 120 through 180. In these cases, correlation is highly significant (better than four MSE) for the solar wind density and pressure and for the IMF magnitude. No correlation effects were found for the solar wind velocity.

It is possible that some degree of correlation is always present between the lower frequency bKOM events and the IMF magnitude and the solar wind density. Figure 11(b), perhaps, suggests that this is the case. However, there is no indication of significant correlation for DOY 1 through 60 from the Voyager 1 data and it seems more likely that the density curve in Figure 11(b) is merely reflecting the rather strong correlation effects occurring during the last 60 days of the whole Voyager 2 period, DOY 20 through 180. The absence of correlation, when higher frequency events or higher average energies are included in the analyses, may be due to contamination by the lower frequencies of the HOM. While the bKOM, the HOM, and the DAM average energies are all well correlated on a time scale of Jovian rotations, the correlation of each emission with solar activity is different (compare Sections 4 and 5).

We note that, in general, the IMF correlation peaks occur a little after epoch for the event analyses while, in the energy analyses, the peaks are before epoch. In each case the displacement of the peak is greater than the positional uncertainty of ± 1 rotation. To interpret this it must be remembered that, although the y–axes in Figures 11 and 12 have been normalized in terms of MSE, they do in fact represent the smoothed averaged magnitudes of each solar wind parameter. We can, therefore, infer the average progress of Jupiter across a sector from the shape of the superposed epoch curves and the positions

of the peaks. Thus it is suggested that the lower frequency bKOM events occur after a sector boundary has passed Jupiter, during the period when the solar wind density and the IMF magnitude are increasing towards the sector centre. Lower energies are emitted soon after the sector has passed. This is demonstrated in Figures 13 and 14. In Figure 13, superposed epoch curves for the period DOY 120 through DOY 180 are extended to longer periods before and after epoch. The IMF minima may then be interpreted as approximate sector boundaries, some 9 days apart, and the maxima as approximate sector centres about 11 to 12 days apart. These values are consistent with the time histories shown in Figure 8. The bKOM activity is shown positioned with respect to a sector in Figure 14. This figure is discussed further in the following section.

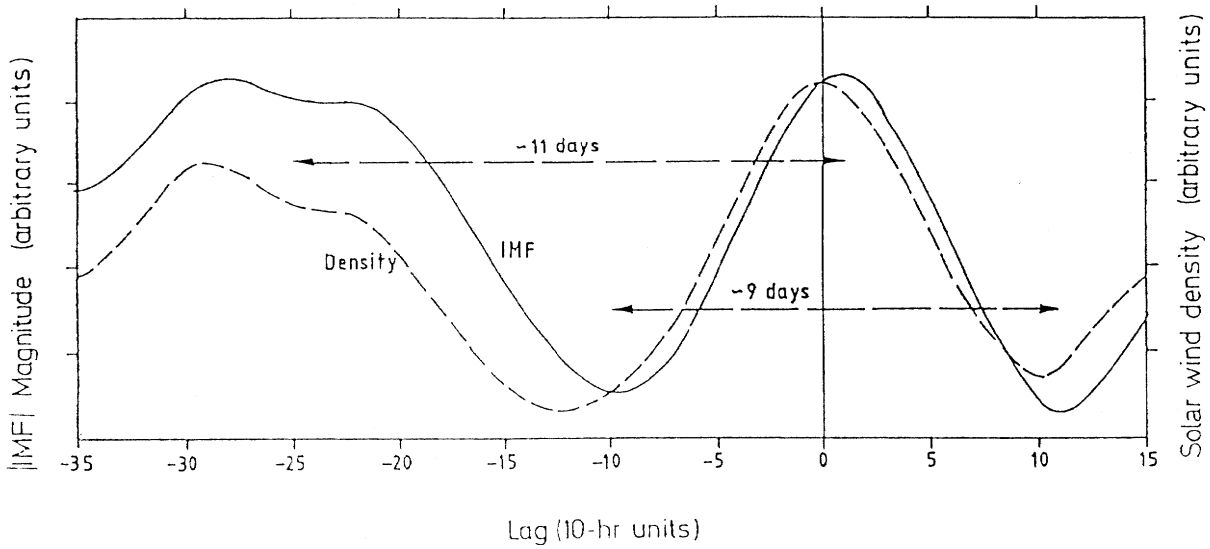

Fig. 13: Smoothed averaged IMF magnitude and solar wind density profiles represented by extended superposed epoch curves for lower frequency (20–310 kHz) events during the period DOY 120 through DOY 180.

7. Discussion

The ideas presented at the end of Section 6 can be further developed, as shown in Figure 14, in which a general picture is suggested of the overall influence of solar activity upon the Jupiter radio emission. In addition to the bKOM, the non–Io DAM and the HOM can also be positioned in relation to the sector from the corresponding superposed epoch diagrams. Thus we can see that, in addition to the bKOM, higher energy HOM tends to be emitted as the sector centre approaches while the non–Io DAM is most likely to occur soon after the sector centre has passed. It is emphasized, however, that this figure is only intended to represent the average trend indicated by the foregoing interpretation of the superposed epoch diagrams.

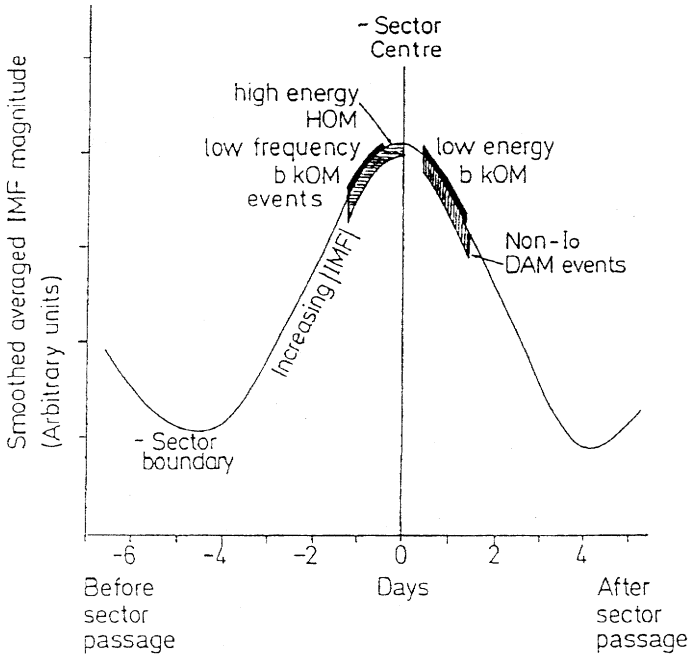

Fig. 14: General picture of solar activity influence on the bKOM, the HOM, and the non–Io DAM, represented by the progress of a sector across Jupiter.

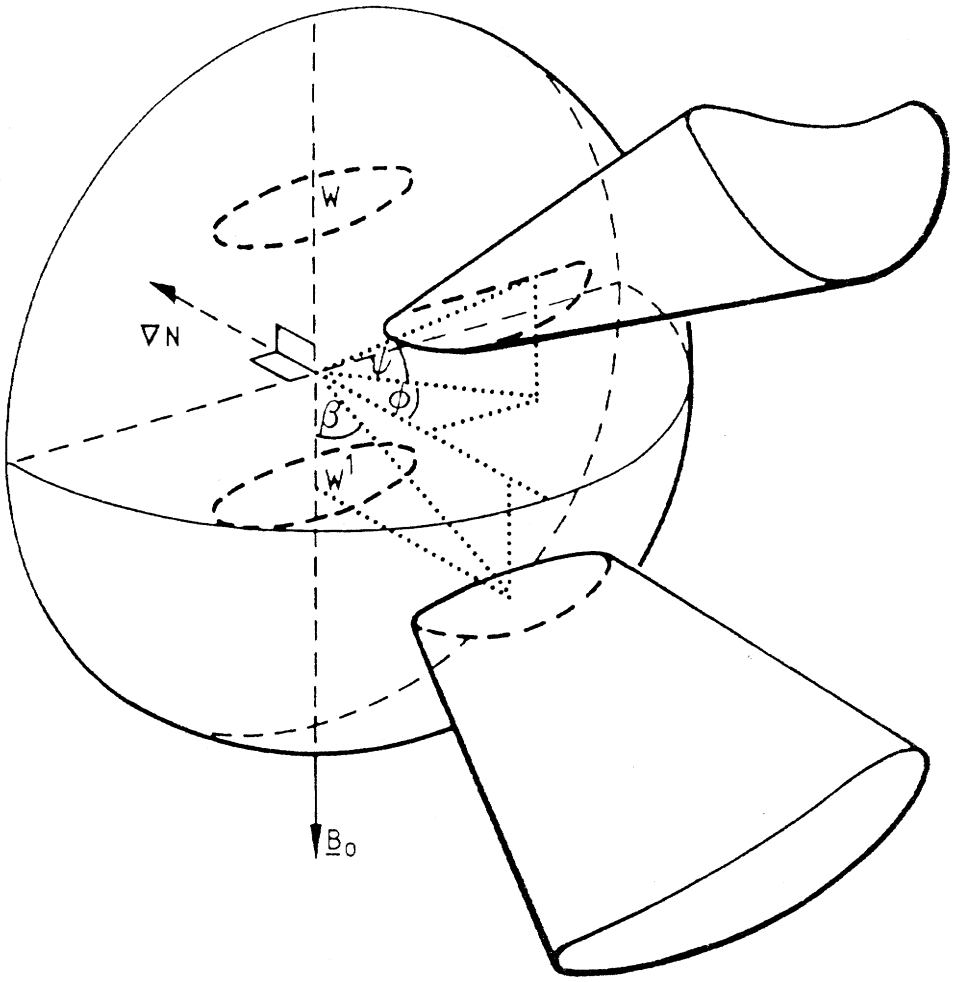

Fig. 15: Sketch of bKOM beaming through radio windows W and W′ (Jones and Leblanc, 1987).

It is not easy to see how the solar wind can interact at Jupiter to influence or to control the radio emission, particularly in the cases of the non–Io DAM and the HOM. A number of parameters inter–correlate with the solar wind density and it may well be that the correlations presented here represent secondary or even tertiary effects. In the case of the bKOM, however, recent work by Jones and Leblanc (1987) locates the source at the outer flank of the Io torus and explains the modulations of activity by a beaming process (Figure 15) which is consistent with the results presented here. According to Jones and Leblanc (1987), the bKOM may be due to linear mode conversion of electrostatic upper hybrid to electromagnetic waves in plasma density gradients. The beaming angle, with respect to the magnetic equatorial plane, depends upon the ratio of the plasma frequency to the gyrofrequency at the source. Thus changes in the electron content of the torus would influence the beaming and the bKOM observed by a spacecraft. If the outer Io torus is compressed in the same manner as the terrestrial plasmasphere during increased magnetic activity, this could increase the density gradient. According to Jones (1986a), an increase in the density gradient in the Io torus would lead to more efficient conversion of the electrostatic upper hybrid waves into the O–mode, thus increasing the probability of bKOM emission.

Acknowledgements: I am grateful to Voyager Principal Investigators H. S. Bridge (Plasma Science Experiment) and N. F. Ness (Magnetometer Experiment) for making data available for the work described in this review. A part of the work was supported by the American Astronomical Society Small Research Grant Program and this is gratefully acknowledged.